



Fatigue assessment of Ti-6Al-4V titanium alloy laser welded joints in absence of filler material by means of full-field techniques

Pasqualino Corigliano, Vincenzo Crupi, Eugenio Guglielmino

University of Messina, Italy

pcorigliano@unime.it, http://orcid.org/0000-0003-0319-048X

crupi.vincenzo@unime.it, http://orcid.org/0000-0001-7498-4733

eguglie@unime.it, http://orcid.org/0000-0001-7793-7406

Carmine Maletta, Emanuele Sgambitterra

University of Calabria, Italy

carmine.maletta@unical.it, http://orcid.org/0000-0002-9204-5358

emanuele.sgambitterra@unical.it, http://orcid.org/0000-0001-5593-399X

Giuseppe Barbieri

Centro Ricerche ENEA Casaccia – Rome, Italy

giuseppe.barbieri@enea.it, http://orcid.org/0000-0001-5583-8634

Fabrizia Caiazzo

University of Salerno, Italy

f.caiazzo@unisa.it

ABSTRACT. The aim of this research activity was to study the fatigue behavior of laser welded joints of titanium alloy, in which the welding was performed using a laser source and in the absence of filler material, by means of unconventional full field techniques: Digital Image Correlation (DIC), and Infrared Thermography (IRT).

The DIC technique allowed evaluating the strain gradients around the welded zone. The IRT technique allowed analyzing the thermal evolution of the welded surface during all the fatigue tests. The fatigue limit estimated using the Thermographic Method corresponds with good approximation to the value obtained from the experimental fatigue tests. The obtained results provided useful information for the development of methods and models to predict the fatigue behavior of welded T-joints in titanium alloy.

KEYWORDS. Fatigue; Welded joints; Marine structures; Digital Image Correlation; Infrared Thermography.



Citation: Corigliano, P., Crupi, V., Guglielmino, E., Maletta, C., Sgambitterra, E., Barbieri, G., Caiazzo, F., Fatigue assessment of Ti-6Al-4V titanium alloy laser welded joints in absence of filler material by means of full-field techniques, *Frattura ed Integrità Strutturale*, 43 (2018) 171-181.

Received: 19.10.2017

Accepted: 05.11.2017

Published: 01.01.2018

Copyright: © 2018 This is an open access article under the terms of the CC-BY 4.0, which permits unrestricted use, distribution, and reproduction in any medium, provided the original author and source are credited.



INTRODUCTION

Titanium alloys, in general, are employed in various applications, ranging from aerospace sector (turbine disks, blades of the compressors, structural elements), passing from the naval sector, to medical and surgical devices [1].

In particular, the Ti-6Al-4V alloy is one of the most widely used, thanks to an excellent combination of low density, high specific strength and corrosion resistance.

Potential applications include also shafts and pressure housings, subsea wellhead and riser components. The first application of titanium alloys in dynamic offshore riser systems was a Taper stress joint (TSJ) [2]. TSJs are specially designed tubular joint sections with a taper over length that permits large deflections of risers on floating production systems, while limiting the bending load transmitted to wellheads or other adjoining structures. The natural flexibility of titanium alloy tubulars derived from a combination of high strength, low elastic modulus (50% of steel), and exceptional air and seawater fatigue resistance and, makes titanium a natural choice for TSJs.

Titanium alloys are also reasonable candidates for low-pressure drilling risers in very deep waters, high pressure drilling risers, and deep water completion and intervention risers. They cost less, and are much more robust, durable, and able to be inspected than composite risers under development. For deep water intervention, titanium alloy risers are sufficiently light to enable small mono-hull vessels (e.g. diving support vessels) to be used for well servicing, offering much lower subsea well maintenance costs.

A Ti-6Al-4V (Ti Gr. 5) alloy drill pipe offers half the modulus of steel, which means twice the flexibility, a high (827 MPa) minimum yield strength, an elevated fatigue strength which is relatively unaffected by the drilling environment and resistance to corrosion and erosion in drill muds and sweet/sour well fluids.

However, given the complex workability of the material with the common techniques, as well as the higher specific cost compared to the most common metallic alloys, the development and tuning of joining techniques suitable to this type of alloys it is undoubtedly one of the factors that most influence the possible dissemination to industrial sectors with lower value added. In this context, the laser weld is considered as an alternative to the traditional techniques to operate the joining of plates of titanium alloys. The main advantages of this process are an increased penetration depth and a reduction of possible welding cracks, and the size of the molten zone with respect to a TIG welding or arc, thus entailing an increase of the mechanical resistance of the welded structures. Innovative methods of welding such as the electron beam have the disadvantage of having to operate in vacuum, in addition, this processing involves the emission of X-rays. However, the welding process induces variations caused also by microstructural factors; in fact, the local mechanical properties of three different areas (base material, BM, heat affected zone, HAZ, welded zone, WZ) will be different [3, 4]. The literature on fatigue analysis of welded joints was reviewed by Fricke [4]. The Recommendations reported in the current Codes, such as International Institute of Welding [5] and Eurocode [6, 7] and also accepted by some of the major Classification Societies of ships and offshore structures, are very conservative.

The assessment becomes more complex in presence of a multiaxial stress state [8-11].

The goal of this research activity was to study the fatigue behavior of laser welded joints of titanium alloy, in which the welding was performed using a laser source and in the absence of filler material, by means of unconventional full field techniques: the digital image correlation (DIC, Digital Image Correlation) and the Infrared Thermography (IRT, Infrared Thermography), in order to analyze the behavior in the surrounding areas of geometric discontinuities and the different material properties. In particular, T-joints were analyzed, obtained from titanium sheets with a thickness of 3 mm and 5 mm, welded by a laser source YB: YAG laser with a maximum power of 10 kW. The fatigue tests were led using loading systems developed ad-hoc and systematic analysis of the results obtained by the DIC and IRT techniques has allowed to better understand the mechanisms of evolution of the local damage within the joints during the application of cyclic loading.

Full-field techniques were already applied by some of the authors have already applied full-field for the assessment of different materials: AA6082 aluminum alloy [12], S355 and high strength steels [13, 14], AISI4140 steel in very high cycle fatigue regime [15], Iroko wood under static loading [16, 17] and shape memory alloys [18].

MATERIALS AND METHODS

Welded joints preparation

The Ti-6Al-4V alloy investigated is of $\alpha + \beta$ type and its chemical composition is shown in Tab. 1, in which it is observed the presence of aluminum that operates as alpha stabilizer and vanadium with the function of beta stabilizer.

A	V	About	N	C	H
<5.5%	<3.5%	<0.2%	<% 00:05	<% 12:08	<0.0375%

Table 1: Nominal chemical composition of the alloy Ti-6Al-4V.

Laser source	Wavelength	Power range	Beam quality	Diameter of the fiber	Spot diameter focus
YB: YAG	1030 nm	1000-10000 W	6 mm * mrad	200 μm	300 pm

Table 2: Features of the laser source.

During welding of titanium alloys, the protection of the molten bath is very problematic because, compared to other materials, titanium has a high affinity with the environmental vapors and gases at high temperatures, which leads to not acceptable characteristics of the weld toe with considerable embrittlement of the same. The importance of this is underscored in the standard AWS D17.1 / D17.1 M: 2010, which provides specifications for fusion welding for aerospace applications.

The welding is prepared in two passes, so that, after the process, the fusion areas in the cross section to the advancing direction of the beam intersect ensuring the continuity of the material (Fig. 1). To achieve these joints, it is necessary that the laser beam is inclined by a suitable angle α (Fig. 2).

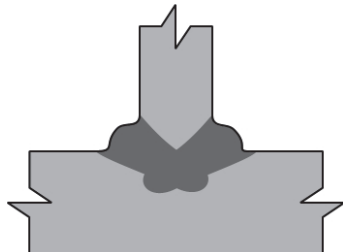


Figure 1: T welding scheme.

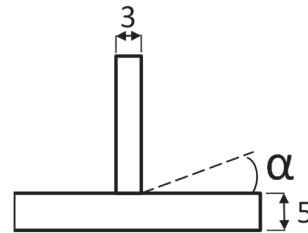


Figure 2: Tilt angle of the laser beam during welding.

Taking into account the high susceptibility to oxidation of titanium alloys at high temperatures, it has been designed and realized in a device ad hoc for the protection and for the mounting of the plates [19].



Figure 3: Protection and clamping system used.

On the basis of previous experience [20] on butt welds, on titanium sheets and on an experimental campaign related to T welded joints, the optimal condition of the process parameters has been identified, shown in Tab. 3.



Power [kW]	Speed [mm/s]	Entry angle [°]
6	80	20

Table 3: Process parameters.

Experimental setup

Experimental measurements were carried out by the use of a servo-hydraulic Instron 8501 machine equipped with a load cell of 100 kN. Each test was led by imposing different values of the maximum load, P_{\max} , in the range between 8 kN and 40 kN, with a load ratio $R = P_{\min}/P_{\max} = 0.1$, considering the run-out at 10^7 cycles and adopting a variable load frequency. In particular, during each test two different frequencies were used, i.e. 0.5 and 5 Hz. The frequency of 0.5 Hz has been adopted to acquire the images to be analyzed using the Digital Image Correlation (DIC) in order to ensure an accurate analysis of the strain field of the specimen, while the frequency of 5 Hz was used to record the temperature increase during the load history by means of the Infrared Thermography (IRT), in order to be able to apply the Thermographic Method [21]. A diagram of the spectrum of the applied load is shown in Fig. 4. In particular, the first two cycles of each test were performed at 0.5 Hz in order to measure the initial state of the specimen, from a point of view of the strain, later cycles at higher frequency (5 Hz), necessary for the thermographic measurements and for the specimen damage, were alternated with low frequency cycles, until failure, as shown in Fig. 4. It is important to observe that, for each step, the effected measuring cycles at 0.5 Hz are only two. This was necessary in order to prevent sudden drops in temperature dictated by the reduction of the frequency of the load, thus compromising the measurement of the thermal history of the specimen by means of the IRT.

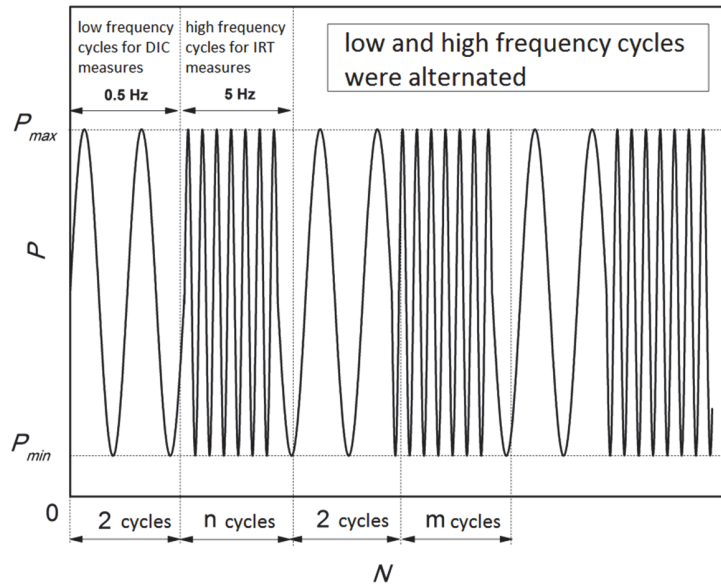


Figure 4: Profile of the applied load to allow IRT and DIC measurements.

In order to ensure the application of the stress in correspondence of only the weld bead, it was designed and created an appropriate loading system (Fig. 5).

During each test, a surface of the specimens has been used to monitor the evolution of the temperature, in correspondence of the welded area, by the use of Infrared Thermography. The opposite side, instead, was used for monitoring the displacements and the relative strains using the optical technique of the Digital Image Correlation.

For this purpose, one side of the specimens was black painted in order to ensure a good surface emissivity ($\epsilon = 0.92$) and, during the test, a series of images at a frequency of 0.2 Hz were acquired in order to trace the evolution of the temperature during the cyclic application of loads. All images were acquired using a thermo-camera (FLIR, A40), characterized by a resolution of 320x256 pixels, and the results were analyzed by using a commercial software (Flir ThermaCAM™ Researcher). On the opposite side of the specimen, however, it has been realized a surface pattern, characterized by an appropriate gray scale in order to allow the digital correlation of the images. The images used for the DIC analysis were

acquired by a digital camera (Sony ICX 625- Prosilica GT 2450 model) with a resolution of 2448 pixels on 2050 and were focused through an optical system consisting of an objective Linos Photonics and a lens Rodagon f .80 mm that, under proper lighting, ensures a resolution of approximately 160 pixels/mm. The correlation of the digital images was performed using a dedicated commercial software (Vic-2D).

The entire experimental setup, adopted during the test, is represented in Fig. 6.

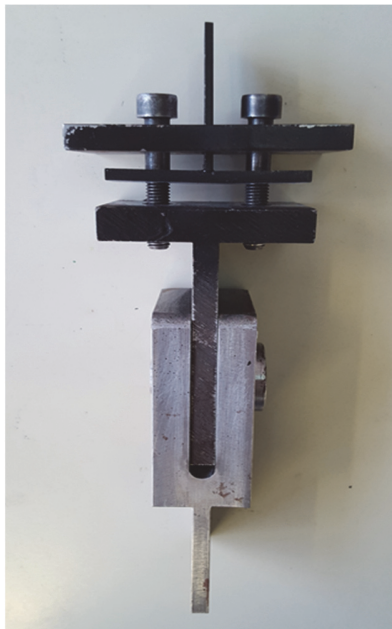


Figure 5: Gripping system of the testing machine.

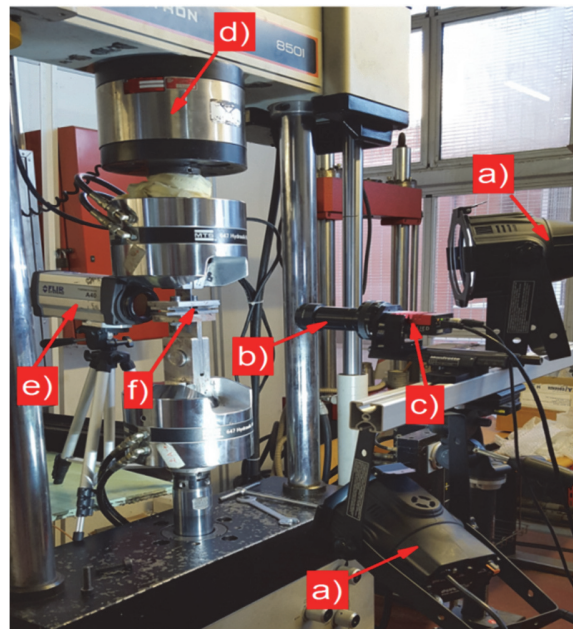


Figure 6: Experimental setup used for testing: a) light source, b) lens, c) camera, d) load cell, e) thermal-camera, f) specimen.

RESULTS AND DISCUSSION

Figs. 7-9 show the maps of the horizontal strain (ε_x), vertical (ε_y) and the maximum principal strains (ε_1), respectively, calculated at the maximum load (40 kN). Specifically, the strains were evaluated taking as a reference image (zero strain), the image acquired at the minimum load of the first cycle of the entire loading history, (Fig. 10). In this way it was possible to identify the process of damage accumulation during the cyclic application of loads. The results show that, by increasing the number of cycles of load applied, the area subject to the maximum strain in the vicinity of the radius of curvature of the weld toe, tends to increase, as index of the growing damage induced on the component.

By thermographic examinations it was possible to investigate the trend of the surface temperature of the specimen, with particular attention to the welded area. As evidenced by thermal images, the modes of failure detected are different. In particular, it has been found that the fatigue cracks are generated in correspondence of the radius of curvature, along the horizontal plate, then propagate initially in the direction perpendicular to the plate itself, and thereafter change direction propagating longitudinally up to the complete break (as shown in Fig. 11, $P_{\max} = 20$ kN). In other cases the cracks are generated from the radius of curvature in the vertical plate, and propagate transversely in the upper joint (Fig. 12, $P_{\max} = 30$ kN). During the tests it was found that the cracks propagate in the surrounding area in which the maximum temperature increase was recorded, which coincides with the areas in which the maximum strain was observed (Fig. 9 and Fig. 12).

The time profile of the temperature, obtained from the infrared images, shows the typical trend of the ΔT -N curve (Fig. 13) that, for higher levels of applied stress, with respect to the fatigue resistance, is characterized by three phases: an initial increase of the temperature (phase I), the maintenance of an approximately constant value of temperature increase ΔT_{AS} (Phase II) and a sudden increase in temperature as soon as the plastic deformations become relevant, bringing the test specimen to fracture (phase III).

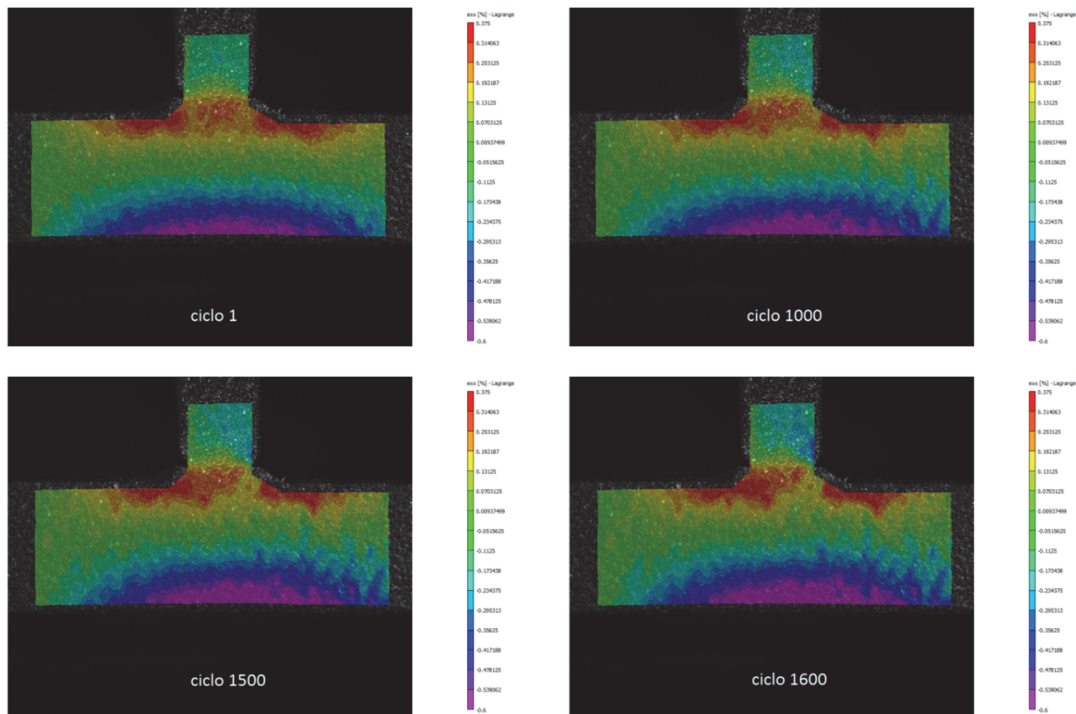


Figure 7: Horizontal strain (ϵ_x) measured at maximum load (40 kN) using the digital image correlation for different load cycles.

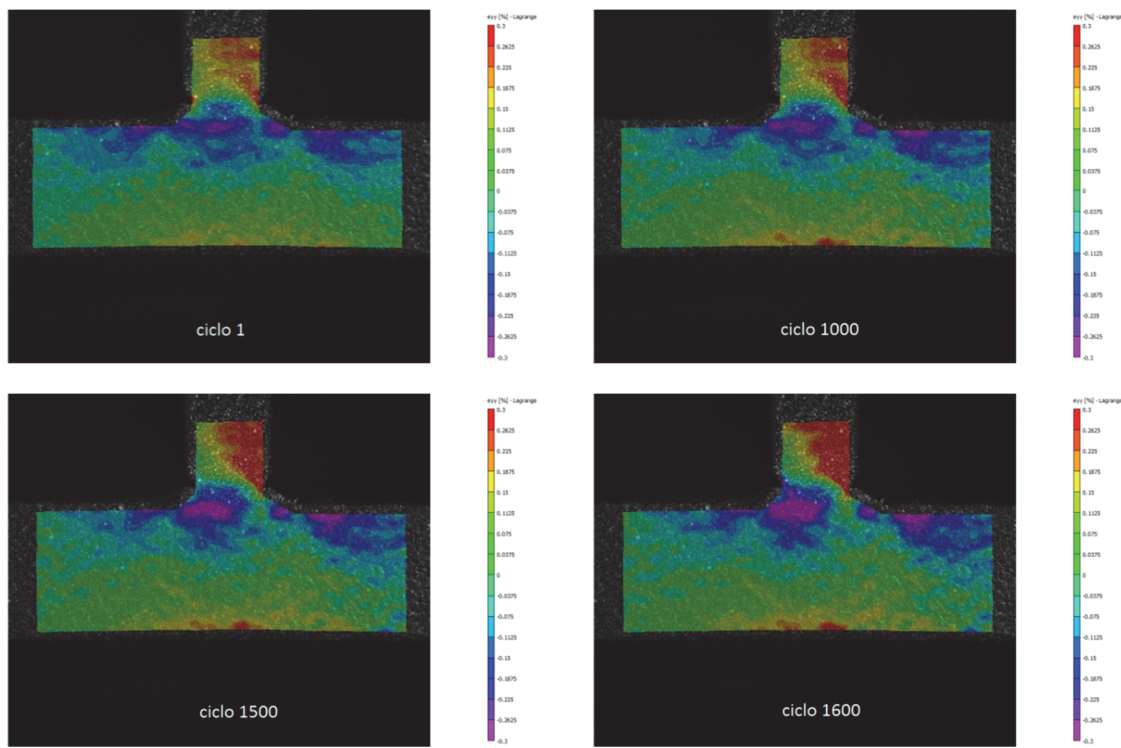


Figure 8: Vertical strain (ϵ_y) measured at maximum load (40 kN) using the digital image correlation for different load cycles.

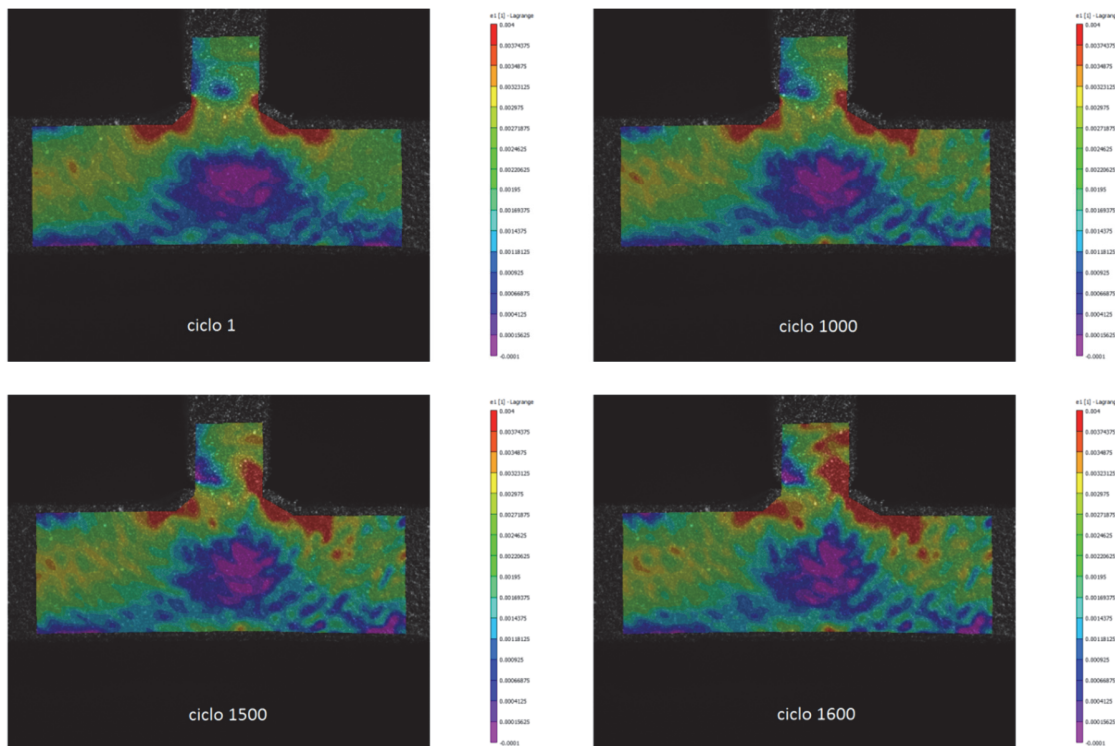


Figure 9: Maximum principal strain (ϵ_1) measured at maximum load (40 kN) using the DIC for different load cycles.

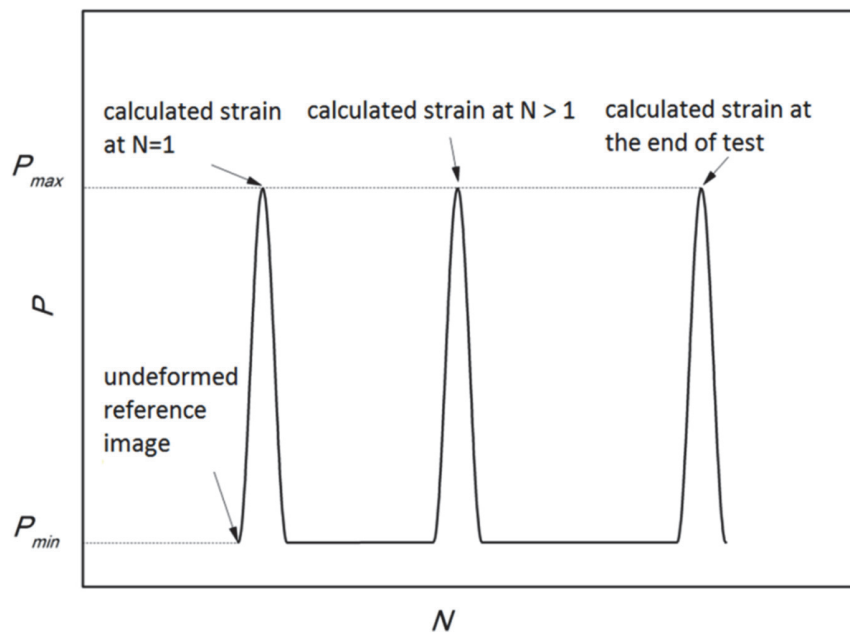


Figure 10: Illustration of the measurements performed to determine the strain around the welded region.

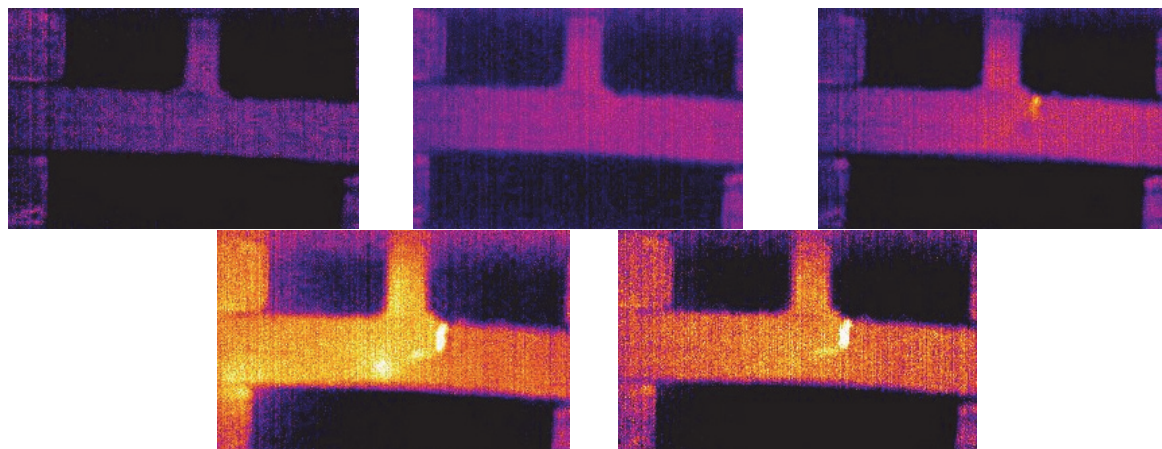


Figure 11: Thermal images during the test at 20 kN.

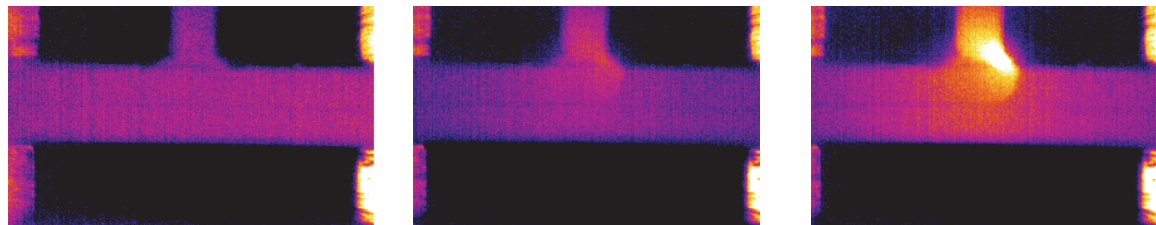


Figure 12: Thermal images during the test at 30 kN.

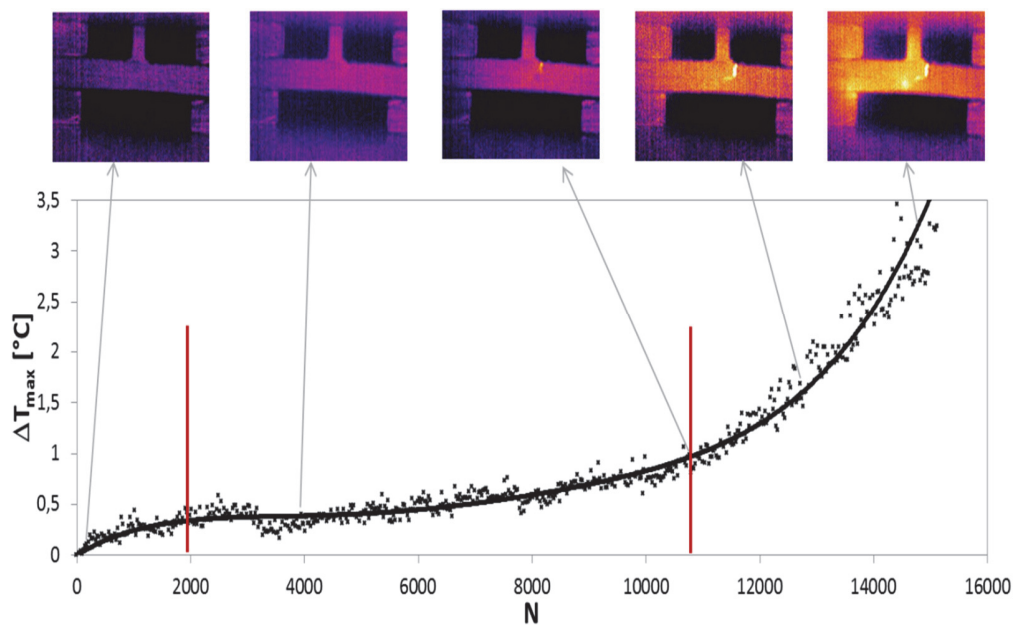


Figure 13: ΔT -N curve during the test at $P_{\max} = 20$ kN.

The Thermographic method, proposed in [21], was also applied, which allowed obtaining a further estimate of the fatigue strength of the Ti-6Al-4V alloy. The stabilized values (stage II) of the temperature increment ΔT_{AS} , above the initial temperature, detected by IR thermography during fatigue testing conducted at $f = 5$ Hz, were plotted as a function of the

square of the corresponding maximum applied load, P_{max}^2 , and the data obtained were interpolated using a linear regression (Fig. 14). The fatigue strength can be estimated by the intersection of the regression line with the abscissa axis; the point located corresponds to the maximum stress below which there is no change in temperature. In the specific case, the fatigue limit P_{max} estimated using the Thermographic Method [21] is about 8.7 kN and corresponds with good approximation to the value identified by the P_{max} - N curve (P_{max} vs number of cycles to failure) obtained from the experimental fatigue tests, see Fig. 15, where the fatigue strength seems to be between 8 kN and 9 kN.

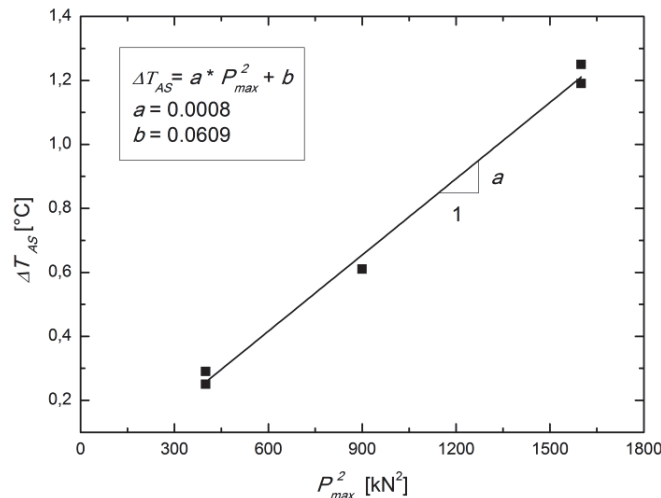


Figure 16: Linear regression values ΔT_{AS} in function of P_{max}^2 .

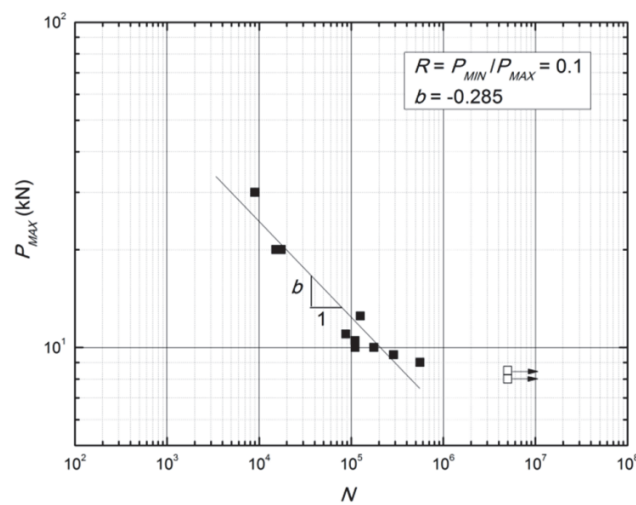


Figure 15: P_{max} – N diagram.

CONCLUSION

The fatigue behavior of titanium welded joints was analyzed, the welding was performed using a laser source and in the absence of filler material. Structural analyses were complemented by full-field investigations, thanks to the use of two non-destructive techniques such as the Digital Image Correlation technique and Infrared Thermography. Specifically, the analysis by means of DIC allowed detecting strain gradients in the surrounding area of the welding and the cumulative damage induced by the loading history. By means of the IRT technique was possible to analyze the evolution of the surface temperature of the welded joints during fatigue tests and apply the Thermographic Method in



order to estimate the fatigue strength of the investigated joint. The results obtained allowed to assess the mode of damage of the component and to provide a first identification of the fatigue strength of the particular joint. In addition, the systematic analysis of the results has provided guidance for the development of methods and models to predict the fatigue behavior of welded joints in T titanium alloy.

ACKNOWLEDGMENTS

The experiments reported in this scientific activity were conducted with the support of research projects PON01_01269 "ELIOS" (Strutture di nuova concezione saldate con laser in fibra") and PON01_02380 "STEM-STELO" ("Sistemi e TEcnologie per la realizzazione di Macchine per lo Sviluppo dei Trasporti Eccezionali e della LOGistica di progetto").

REFERENCES

- [1] Schutz, R.W., Watkins, H.B., Recent developments in titanium alloy application in the energy industry, *Materials Science and Engineering: A*, 243 (1998) 305–315.
- [2] Schutz, R. W., Baxter, C. F., Boster, P. L., Fores, F. H., Applying titanium alloys in drilling and offshore production systems. *JOM*, 53 (2001) 33-35
- [3] ASM Metals handbook, Welding, Brazing and Soldering, ASM International, 6 (1993).
- [4] Fricke, W., Recent Developments and Future Challenges in Fatigue Strength Assessment of Welded Joints, Special Issue "Fatigue Design and Analysis in Transportation Engineering", *P I MechEng C-J Mech*, 229 (2015) 1234-1249.
- [5] International Institute of Welding. Fatigue design of welded joints and components. Abington Publishing, Abington, Cambridge, (1996).
- [6] Eurocode 3. Design of steel structures: part 1-1: general rules and rules for building. European Committee for Standardisation, (1993).
- [7] Eurocode 9. Design of aluminium structures, part 2: structures susceptible to fatigue. Brussels, Belgium: European Committee for Standardisation, (1999).
- [8] Susmel, L., Multiaxial Notch Fatigue: from nominal to local stress-strain quantities. Woodhead & CRC, Cambridge, UK, 582 (2009).
- [9] Sonsino, C.M., Multiaxial fatigue assessment of welded joints, Recommendations for design codes, *Int J Fatigue*, 31 (2009) 173-187.
- [10] Susmel, L., Nominal stresses and Modified Wöhler Curve Method to perform the fatigue assessment of uniaxially loaded inclined welds, *P I Mech. Eng. C – J. Mec.*, 228 (2014) 2871-2880.
- [11] Susmel, L., Taylor, D., A critical distance/plane method to estimate finite life of notched components under variable amplitude uniaxial/multiaxial fatigue loading, *Int J Fatigue*, 38 (2012) 7–24.
- [12] Faraji, A.H., Goodarzi, M., Seyedein, S.H., Maletta, C., Effects of welding parameters on weld pool characteristics and shape in hybrid laser-TIG welding of AA6082 aluminum alloy: numerical and experimental studies, *Welding in the World*, 60 (2016) 137-151.
- [13] Corigliano, P., Crupi, V., Epasto, G., Guglielmino, E., Risitano, G., Fatigue assessment by thermal analysis during tensile tests on steel. *Procedia Eng*, 109 (2015) 210 – 218.
- [14] Corigliano, P., Epasto, G., Guglielmino, E., Risitano, G., Fatigue analysis of marine welded joints by means of DIC and IR images during static and fatigue tests. *Eng. Fract. Mech.* 183 (2017) 26–38.
DOI:10.1016/j.engfracmech.2017.06.012.
- [15] Crupi, V., Epasto, G., Guglielmino, E., Risitano, G., Analysis of temperature and fracture surface of AISI4140 steel in very high cycle fatigue regime, *Theoretical and Applied Fracture Mechanics*, 80 (2015) 22 - 30.
- [16] [Bucci, V., Corigliano, P., Crupi, V., Epasto, G., Guglielmino, E., Marinò, A., Experimental investigation on Iroko wood used in shipbuilding, *P. I. Mech. Eng. C-J. Mec.*, 231 (2017) 128 – 139.
- [17] Corigliano, P., Crupi, V., Epasto, G., Guglielmino, E., Maugeri, N., Marinò, A., Experimental and theoretical analyses of Iroko wood laminates; *Compos. Pt. B – Eng.*, 112 (2017) 251 – 264.
- [18] Maletta, C., Bruno, L., Corigliano, P., Crupi, V., Guglielmino, E., Crack-tip thermal and mechanical hysteresis in Shape Memory Alloys under fatigue loading. *Mater Sci Eng A: Struct*, 616 (2014) 281–287.



-
- [19] Caiazzo, F., Sergi, V., Corrado, G., Alfieri, V., Cardaropoli, F., Apparatus automated laser welding, Patent SA2012A000016 University of Salerno (2012).
 - [20] Caiazzo, F., Alfieri, V., Conrad, G., Sergi, V., Investigation and optimization of laser welding of Ti-6Al-4V titanium alloy plate, *Journal of Manufacturing Science and Engineering, Transactions of the ASME*, 135 (2013).
 - [21] La Rosa, G., Risitano, A., Thermographic methodology for rapid determination of the fatigue limit of materials and mechanical components, *Int J Fatigue*, 22 (2000) 65 - 73.